Automatic segmentation of skin regions in thermographic images: an experimental study

CRISTINA M.R. CARIDADE
Polytechnic of Coimbra, ISEC, Coimbra, PORTUGAL
Department of Physics and Mathematics
Applied Research Institute, Laboratory for Applied Biomechanics, Coimbra, Portugal
CICGE - Centro de Investigação em Ciências Geo-Espaciais, Porto, PORTUGAL

LUIS ROSEIRO
Polytechnic of Coimbra, ISEC, Coimbra, PORTUGAL
Department of Mechanical Engineering
Applied Research Institute, Laboratory for Applied Biomechanics, Coimbra, PORTUGAL
CEMMPRE - Centre for Mechanical Engineering, Materials and Processes, Coimbra, PORTUGAL

Abstract: Infrared thermography can be applied in medical applications, such as monitoring skin temperature in inflammatory processes. The possibility for health care professionals and patients to be able to easily, quickly and economically, at anytime and anywhere, monitor the skin temperature distribution through the acquisition of images to control skin infections is extremely important nowadays.
This work aims to develop an automatic methodology for the segmentation, identification, analysis and diagnosis of skin inflammation based on thermographic images. The study compares thermographic images from sub-regions of the hand skin and presents an experimental investigation to segment and identify features in the images automatically. Left and right-hand images from two volunteers' obtained in different conditions, such as cold action, activity action (opening and closing the hand), and friction action (rub both hands), were considered and analyzed. The obtained results demonstrate the feasibility of the implemented procedures and encourage developing and implementing an operating system to monitor skin infections in thermographic images.

Key-Words: Thermography; Image processing; Segmentation; Skin inflammation; Monitoring skin temperature

Received: January 10, 2021. Revised: July 5, 2021. Accepted: July 25,2021. Published: August 2, 2021.

1 Introduction

Infrared thermography is a technic that can be used in a process as long as the temperature is measurable [1]. Thermography has been implemented in a wide range of areas, as it is a non-invasive examination technology, with nondestructive characteristics. Initially used for specialized military purposes, this technique has evolved through development and refinement. Currently, it is a technology that can apply in civil construction, automotive and metallurgical industry, electrical and mechanical installations, aeronautics, surveillance, and security systems, among others [1]. More recently and as a noninvasive technology, thermography has been increasingly applied in medicine, particularly to evaluate body tissues and fluids [2]. Thermography is an image based technique, which allows the observation of human body skin temperature distribution [3]. Being a low-cost, noninvasive technique that does not emit radiation, it becomes an imaging method with numerous medical applications [4, 5]. It has been used as a complementary tool for the detection of breast cancer and in the assessment of burns [6, 7, 8]. In the diagnosis of inflammatory processes, it becomes very useful in detecting and monitoring the therapeutic procedures [9, 10, 11]. Thermography allows the definition of superficial thermal patterns of a patient through equipment that allows obtaining visual and quantitative information of the distribution of body temperatures [12]. This technology also allows the acquisition of information about the normal or abnormal functioning of the sensory system, vascular function, muscle trauma, and inflammation. Furthermore, by using a portable and reliable instrument capable of visualizing, analyzing and evaluating the temperature distribution of skin surfaces, the monitoring of skin infections can be controlled by all health care professionals or even by the patients themselves. Modern portable thermal image cameras, like Seek CompactXR, are small, light and easy to use and can be used to acquire

thermal images of the skin surface.

This work presents an experimental study to compare skin temperature distribution using thermal images obtained by a low-cost portable camera. The objective is to compare thermographic images after the application of controlled activity in a skin region and to evaluate patterns compared to the reference of temperature distribution maps from control situations. The obtained results show a way to develop and implement an innovative, noninvasive, cheap and reproducible method to detect the thermal map distribution of the skin and the differences, allowing the identification of the presence of skin inflammation. The study is part of the research line for implementing a complete system accessible to any health professional to monitor skin inflammation in bedridden, diabetic or other patients. The inflammatory process is evident, and that can be quickly and accurately controlled.

2 Material an methods

The implemented experimental work was considered images taken using a low-cost, portable Seek CompactXR (Seek Thermal, Inc., CA) thermal camera with a sensor of 206 × 156. The camera has a focusable lens, a field of view of 36°, and an operating temperature range between −40◦ C to 330◦ C. Acquired images was taken in an acclimatized packed room, with controlled temperature, relative humidity less than 50%, absence of light, equipment away so that photographed the entire hand. The volunteer's hand placed in a smooth and homogeneous wooden surface. Live colour explicit photographs were taken in RGB (R-red, G-green and B-blue) colour model, and the images were stored in JPEG (Joint Photographic Experts Group) standard image format with 720 × 1280 pixels in size.

For the implementation of the work, two healthy volunteers were used, who was duly informed of the intended objectives, providing free, informed and written consent. The study did not involve the collection of any personal data from the volunteers.

In the acquisition protocol, each volunteer was seated and rest for 15 minutes in the collection room to be acclimatized. Firstly, several images were taken at the beginning of the test from the left hand and the right hand. The hand was placed on a neutral surface to avoid external effects due to contact with the hand skin. After, the hand of the volunteer was placed in contact with a controlled cold surface for 2 minutes and several images were taken. After, the volunteer was asked to perform the activity of opening and closing the hand as also the friction between the two hands. Fig.1 shows four different images of the right hand (A, B, C and D) of volunteer 1 (V1) and volunteer 2 (V2).

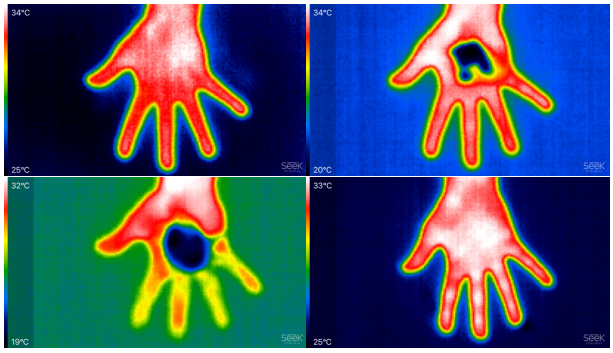

Figure 1: Examples of thermography images obtained from direct hand skin photographs: A, B, C and D.

The images were processed with algorithms developed in Matlab Software, Version 7 (Math-Works, Natick, MA, USA).

The methodology used has three separate stages: Image Pre-processing, Images alignment, and Images comparison represented in the flowchart of Fig.2. The first stage is applied to each image and consists of eliminating the temperature bar, automatically recognize the maximum and minimum temperature, convert to a grayscale image, cropping the image and converting it to an indexed image. In the second stage and after the first stage is applied to the two images, it is necessary to align the pair. Thus, geometric transformations are applied to the second image in order to be as aligned as possible to the first one. In the third and last stage, the difference between the pair of images is calculated, the regions of interest (ROIs) are segmented, and the characteristics of these regions are calculated.

2.1 Images Pre-processing

In the pre-processing, each image is automatically applied a set of techniques and methodologies. Initially, the temperature bar on the left side of the thermographic image (Fig.3) is separated and the maximum (upper left corner) and minimum (lower left corner) temperature values are recognized using optical character recognition, all automatically (Fig.3).

After converting the image to grayscale, the next step is to crop the image so that the region of interest (hand) occupies the entire image. In Fig.4 it is possible to observe this transformation made to the image A1 and B1 of Figure 3, obtaining the image GA2 and GB2, using the same methodology described in [13]. Finally, it is necessary to convert the grayscale image to an indexed image so that each intensity corresponds to a temperature. Therefore, the pixel intensity values (I) represented by a integer number between 0 and 255 are scaled between 0 and 1 and then adjusted between the minimum (min) and maximum (Max)

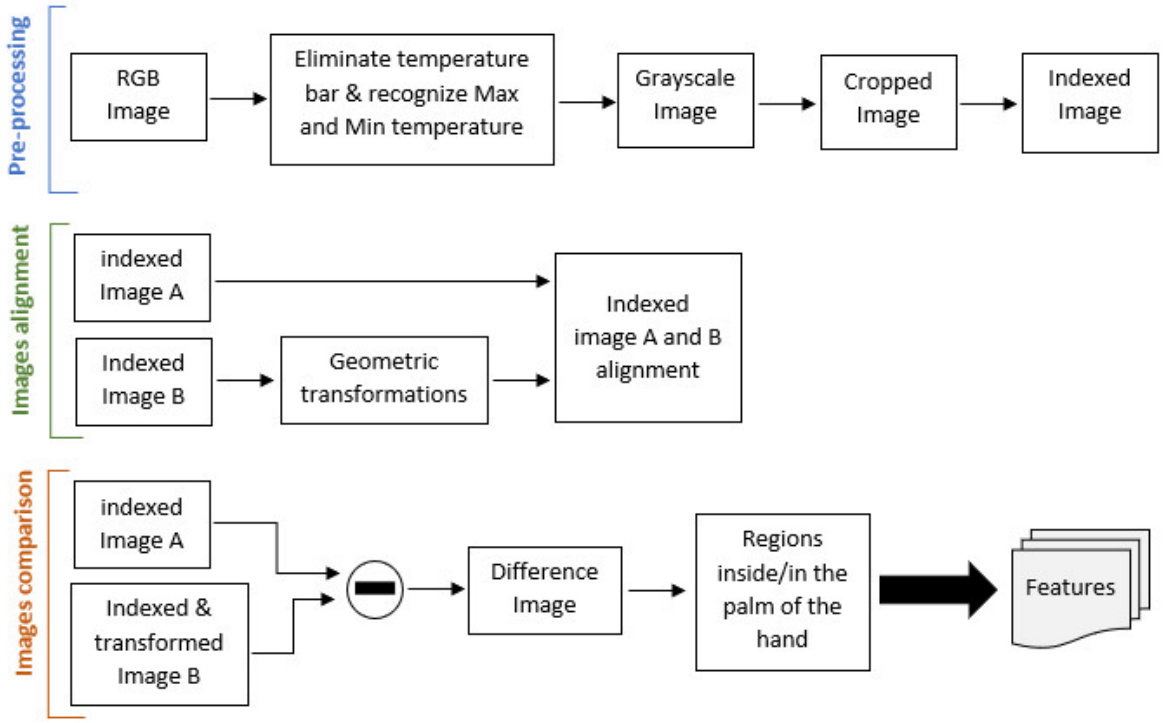

Figure 2: Flowchart of the steps followed in the applied methodology.

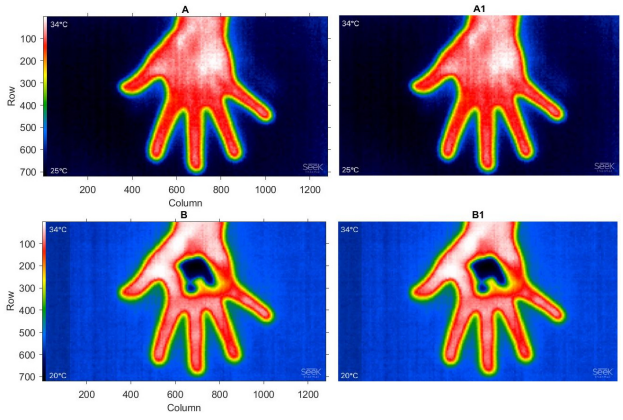

Figure 3: Original RGB images A (top), B (down) and without temperature bar A1 and B1 respectively.

temperature of each image by equation 1.

$$T = min + (Max - min) \times \frac{I}{256}, \qquad (1)$$

As an example, in the IA2 image the pixel intensities vary between 24°C and 34°C while in the IB2 image they vary between 20°C and 34°C. Therefore, a pixel of intensity 128 in image A corresponds to a temperature of 29ºC while the same pixel in image B corresponds to a temperature of 27ºC. In Fig.4 on right are represented the corresponding indexed images (IA2 and IB2) with the intensity of grey tones associated with temperature.

2.2 Images alignment

After the pre-processing and starting from two images of the same hand, taken at different times, it is necessary to align the two images to establish comparisons. A set of control points in the first indexed image and the corresponding ones in the second indexed image are used to infer the geometric transformation or set of geometric transformations (translation, rotation, scaling) that must be apply to adjust the two images [15]. Fig.5 on the left shows the two superimposed images without any type of alignment (IA2 & IB2) and on the right after the IB2 image has undergone geometric transformations, obtaining IB3, to align this image with the IA2 image (IA2 & IB3).

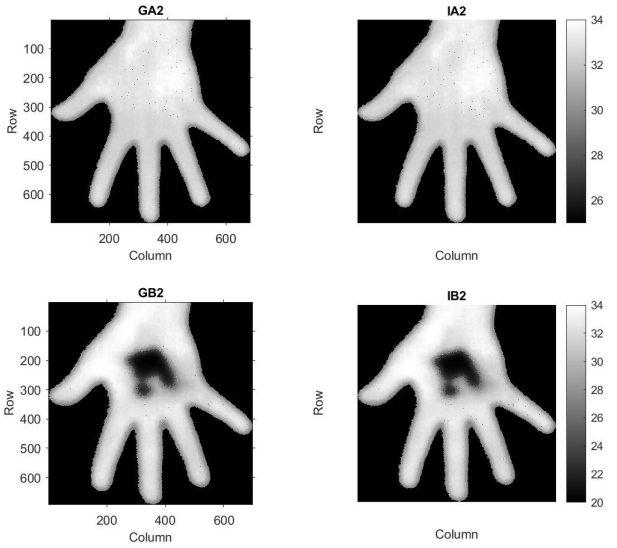

Figure 4: Grayscale cropped images GA2 and GB2 (left) and indexed image IA2 and IB2 (right).

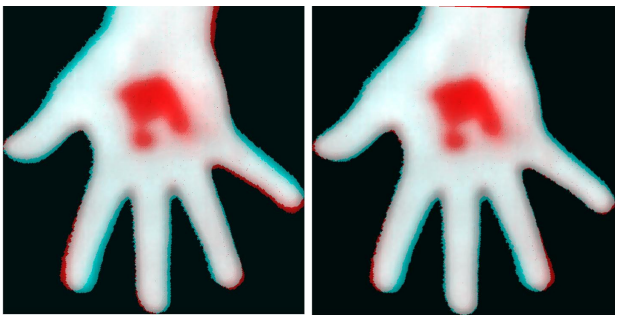

Figure 5: Images superimposed: IA2 & IB2 (before alignment-left) and IA2 & IB3 (after alignment-right).

In Fig.5 the regions defined in red are regions where there are differences between the two images.

2.3 Images comparison

With the regions that define the difference between the two established images (Fig.6 (left top)), it is possible to identify only those regions that are found in the palm automatically. For this, the image of the absolute difference between the two images (Fig.6 (left top)) was converted to a black and white image, applying the Otsu method [14] and only the palmar region was selected (Fig.6 (right top)) using the procedures described in [13]. Then, the noise was eliminated using morphological erosion operators, with a structuring element with 2-pixel radius disk shape (Fig.6 (left down)). Small regions (less than 200 pixels) and regions near the edges of the images were eliminated and the holes were filled (Fig.6 (right down)).

The bounding box was defined with the detected

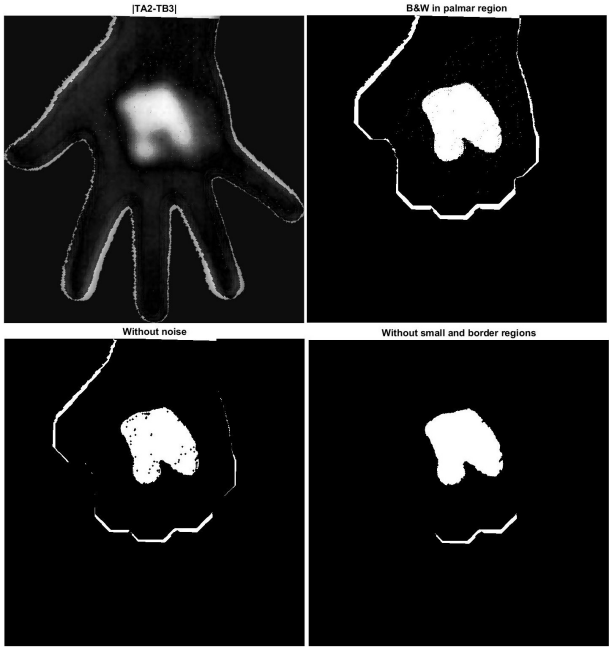

Figure 6: $|IA2 - IB3|$ image (left top) black and white representation in palmar region (right top) without noise (left down) and without small and border objects (right down).

regions, and only the regions whose bounding boxes are fully inserted in the palm of the hand were selected. In Fig.7 two regions were found, but only the area limited by green colour is inside the palm of the hand, so only this region will be selected.

After detecting the regions of difference between the two images in the palm, some region features will be calculated. The maximum, minimum, average and standard deviation temperature of the region and the number of pixels are calculated. In Fig.8 it is possible to visualize the detected region in the IA2 image and in the IB3 image. In this case, the area has 20353 pixels. The maximum, minimum, average and standard deviation temperature of this region in the IA2 image are: 33.21ºC, 25ºC, 30.73ºC, 2.96 and in the IB3 image are: 33.69ºC, 19.56ºC, 28.97ºC and 4.85.

3 Experimental tests

Some experimental tests were implemented with only two volunteers, using the left hand (l) and the right hand (r) by the action of cold (C), activity (A) and friction (F) at moments 0, 1 and 2 minutes. The photos were taken of two volunteers (V1 and V2) at the beginning of the test on the left hand (l0) and on the right hand (r0), after 1 minute and 2 minutes in the presence of cold for the left hand (Cl1 and Cl2) and for the right hand (Cr1 and Cr2), after 1 and 2 minutes by the activity of opening and closing the hand for the left hand (Al1 and Al2) and right hand (Ar1 and

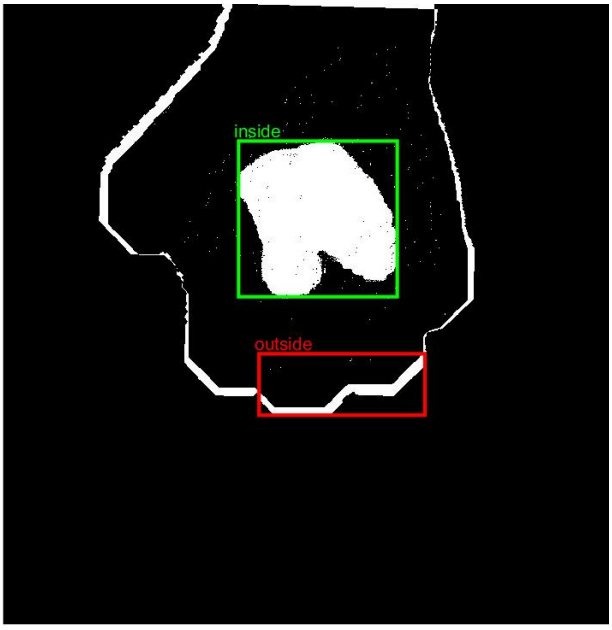

Figure 7: $|IA2-IB3|$ image with the detected region: inside region (green) and outside region (red).

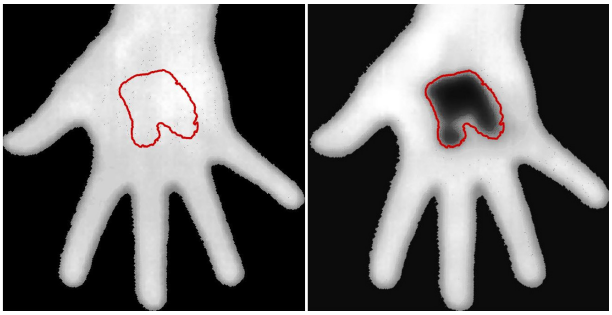

Figure 8: Two images for comparation: A and B .

Ar2) and after 1 and 2 minutes of friction between two hands for the left hand (Fl1 and Fl2) and for the right (Fr1 and Fr2). Thus, 21 tests were developed by comparing pairs of images without repetition of a volunteer's right hand (r0, Cr1, Cr2, Ar1, Ar2, Fr1, Fr2). Another 21 tests for the left hand (l0, Cl1, Cl2, Al1, Al2, Fl1, Fl2), and for the two volunteers, i.e. a total of 84 tests. All tests were generated automatically and values were collected for analysis.

4 Results

In the tests performed by the action of cold, the regions were easily defined and it was possible to acquire the features of these regions in comparison with other situations. Fig.9 shows an example of the comparison of the image subjected to cold for 2 minutes (Cr2) with the remaining images of the right hand of volunteer V1. The selected regions on the palm have different sizes from the smallest with 6098 pixels (Cr2 vs. Cr1) to the largest with 30983 pixels (Cr2 vs. Ar2) with a marked variation in the minimum temperature (between 18°C and 25°C) and the average temperature (between 24°C and 30°C) but a maximum temperature variation of less than 1°C.

Suppose it is analyzed, for example, the left hand of volunteer V2 and compare the image by cold at 1 minute (Cl1) with the remaining ones. In that case, the graphs represented in the Fig.10 are obtained. In blue are defined the temperatures of the palmar subregion of the image Cl1 and orange the corresponding temperatures of these subregions in the other images. Regarding the minimum temperature, it is verified that it is always lower in Cl1 than all the other images. The most significant (smallest) difference will be between the Cl1 and Al2 (Cl2) image, which was to be expected. In relation to the maximum temperature, it is also consistently lower in the Cl1 image than the others, except the Cl2 image (cooled to 2 minutes). The most significant difference is found in pair Cl1, I0, and the smallest in pair Cl1, Cl2. As for the comparison between the average temperatures of pairs of images in the palm subregions, they have a behavior similar to that of the maximum temperatures: the distance (Cl1, Cl2) is negative and is the shortest distance and the most significant distance is in the pair (Cl1, l0). These results are similar in the identical tests (left/right hand of volunteer V1 or right hand of volunteer V2).

In tests by activity or friction action, the temperature difference was not felt in localized regions. Hence, no subregions of the palm were automatically detected, but the palm region as a whole was analyzed. Table 1 presents the calculated features for comparing the image of the initial right hand (r0) with the images after the activity (Ar1, Ar2) and friction (Fr1, Fr2) of the volunteer V1. It was verified that

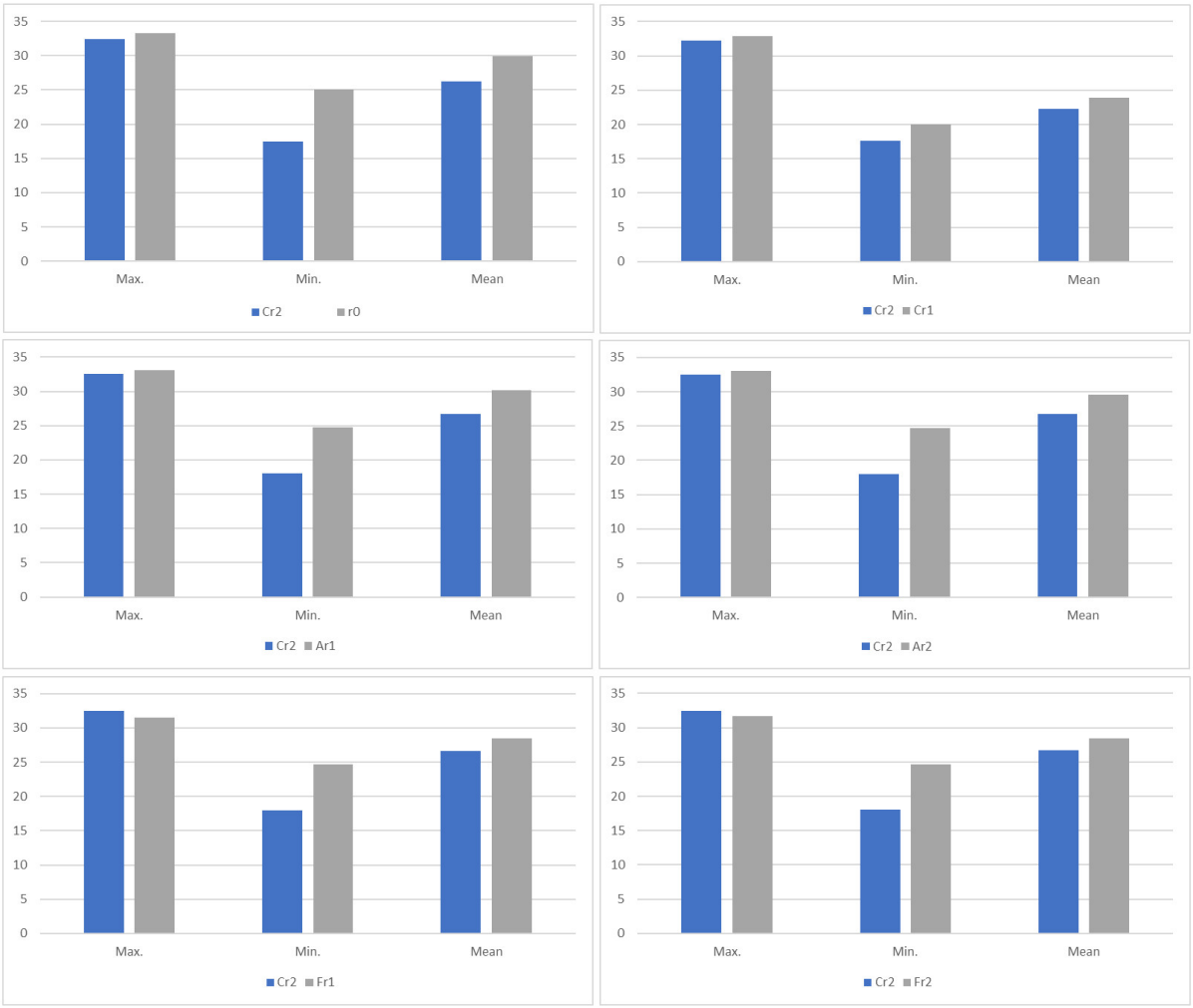

Figure 9: Features of the right hand palmar subregion of volunteer V1 by cold action.

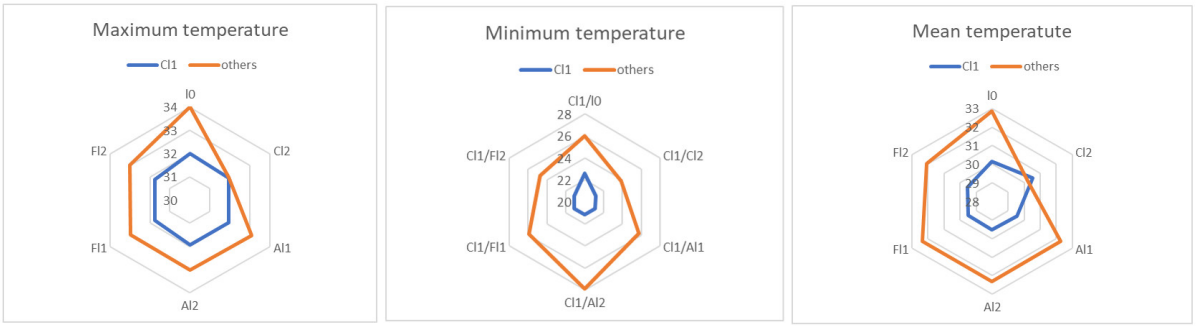

Figure 10: Features of the right hand palmar subregion of volunteer V1 by cold action.

the number of pixels in the palmar region of volunteer 1's right hand varies by approximately 9.5%. The maximum, minimum and mean temperature varies in 1.86ºC, 2.27ºC and 1.86ºC respectively. The standard deviation of the palmar region ranges from 0.83 in the r0 image to 1.04 in the Ar1 and Ar2 image. Thus, the heat is barely visible in the activity action and in the friction action since the maximum and minimum temperatures remain practically constant, only the average temperature is 1ºC higher in the activity in relation to the friction. These results are similar in the identical tests (left/right hand of volunteer V2 and left hand for volunteer V1).

Table 1: Right hand palm region features of volunteer V1 by the action of activity and friction

Image	#	Max.	Min.	Mean	Std
r0	134559	34.00	26.60	32.77	4.85
Ar1	148673	33.36	24.33	32.15	1.04
Ar2	138776	33.41	24.45	31.90	1.04
Fr1	143599	32.30	24.50	31.12	0.87
Fr2	142558	32.14	24.44	30.91	0.90

5 Conclusion

A set of image processing techniques and methodologies were automatically applied to thermographic images of the skin hand to find regions of skin inflammation. The regions were identified by comparing pairs of images that were segmented, and some features were extracted, such as the minimum, mean and maximum temperature, and the standard deviation. Eighty-four (42 on the right hand and 42 on the left hand) comparisons were made between thermographic images of two volunteers. Images were acquired in 3 different situations (by the action of cold, by activity and by friction) during 1 or 2 minutes. The results obtained from this experiment study allow to verify that the segmentation and identification of skin thermographic maps where the inflammation exists is a possible technique that can be applied as a way to monitor or prevent skin infections, such as in the case of diabetic foot or pressure ulcers in bedridden patients. The methodology compares images from the same region. Overall, it can be stated that the results are encouraging. Still, more work is needed to develop an operational system to identify, segmentation and monitor skin lesions in thermographic images. Shortly, real studies will have to be carried out with thermographic images of skin regions with and without inflammations in patients to assess the techniques and methodologies of image processing developed and the features that must be extracted to describe the skin region in question. The complete and operational system to monitor and prevent skin infections will also be developed in parallel.

References:

[1] Gonçalves, T. (2011). Análise de Sistemas de Energia e Máquinas Eléctricas com Recurso a Termografia. Master's thesis from Faculdade de Engenharia da Universidade do Porto. https://repositorio-aberto.up.pt/bitstream/10216/62082/1/000149319.pdf

[2] Lahiri, B B et al. Medical applications of infrared thermography: A review. Infrared physics & technology vol. 55,4 (2012): 221-235. doi:10.1016/j.infrared.2012.03.007

[3] García, A., Camargo, C., Olguín, J., Barreras, J.A.L., Analysis of risk for repetitive work using thermography sensory. *Advances in Intelligent Systems and Computing*, N0.590, 2018, pp. 239–248. https://doi.org/10.1007/978-3-319-60483-1_24

[4] Garcia, L., Vergara, L. (n.d.). A Termografia como instrumento de avaliação em Ergonomia Thermography as an ergonomic tool of assessment.

[5] Neves. (2012). Diagnosis of RSI - WMSD handle by Thermography [Avaliação da aplicação da termografia no diagnóstico de LER-DORT de punho]. XXIII Congresso Brasileiro Em Engenharia Biomédica – XXIII CBEB, November 2015, 583–586. https://doi.org/10.13140/2.1.1644.0642

[6] Sarigoz, T., Ertan,T. Role of dynamic thermography in diagnosis of nodal involvement in patients with breast cancer: A pilot study, Infrared Physics & Technology, Volume 108, 2020, https://doi.org/10.1016/j.infrared.2020.103336.

[7] Abdulla, M. et. al, A Systematic Review of Breast Cancer Detection Using Thermography and Neural Networks, IEEE Access, vol. 8, pp. 208922-208937, 2020.

[8] Nguyen, A.T., Chamberlain, K. Holland, A.J. Paediatric chemical burns: a clinical review. Eur. J. Pediatr. 180, 1359–1369 (2021). https://doi.org/10.1007/s00431-020-03905-z

[9] Hutting, K.h. et. al Infrared thermography for monitoring severity and treatment of diabetic foot infections. Bioscientifica Ltd, Volume 2, Issue 1,Pages 1-10 (2020). https://doi.org/10.1530/VB-20-0003

[10] Kasprzyk-Kucewicz, T., Cholewka, A., Bałamut, K. et al. The applications of infrared thermography in surgical removal of retained teeth effects assessment. J Therm Anal Calorim 144, 139–144 (2021). https://doi.org/10.1007/s10973-020-09457-6

[11] Souza, A.K.L., Colares, R.R., Souza, A.C.L., The main uses of ozone therapy in diseases of large animals: A review, Research in Veterinary Science, Volume 136, 2021, Pages 51-56, https://doi.org/10.1016/j.rvsc.2021.01.018.

[12] Usamentiaga, R. , Venegas, P. , Guerediaga, J. , Vega, L. , Molleda, J. , Bulnes, F. (2014). Infrared thermography for temperature measurement and non-destructive testing. Sensors, 14(7), 12305–12348. https://doi.org/10.3390/s140712305

[13] Caridade C.M.R., Roseiro, L., Skin temperature classification by Image Processing, 2021 16th Iberian Conference on Information Systems and Technologies (CISTI), 2021, pp. 1-6, doi:10.23919/CISTI52073.2021.9476646.

[14] N. Otsu, A threshold selection method from greylevel histograms. *IEEE Trans. Systems Man, and Cybernetics*, Vol. 9, 1979, pp. 62-66.

[15] Gonzalez R.S., Woods R.E., Digital image processing. Third Edition, Prentice Hall, New Jersey, 2008.

Contribution of individual authors to the creation of a scientific article (ghostwriting policy)

Cristina Caridade implemented the Algorithm in Matlab and was responsible for the statistical analysis.
Luis Roseiro carried out the simulation and has organized and executed the experiments.

Follow: www.wseas.org/multimedia/contributor-role-instruction.pdf

Creative Commons Attribution License 4.0 (Attribution 4.0 International , CC BY 4.0)